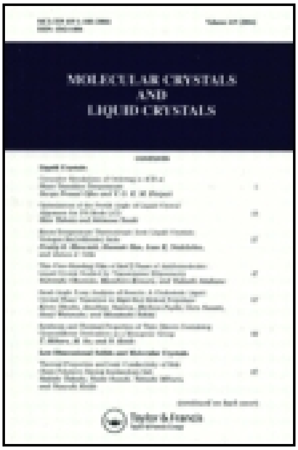

Molecular Crystals and Liquid Crystals
Publication details, including instructions for authors and subscription information:
http://www.tandfonline.com/loi/gmcl16

The Dynamics of the Formation of a Periodic Deformation in a Lyotropic Liquid Crystal

J. P. McClymer [a] & M. M. Labes [a]

[a] Department of Chemistry, Temple University, Philadelphia, PA, 10122

Version of record first published: 21 Mar 2007.

Mol. Cryst. Liq. Cryst., 1987, Vol. 144, pp. 275–283
Photocopying permitted by license only

Printed in the United States of America

The Dynamics of the Formation of a Periodic Deformation in a Lyotropic Liquid Crystal

J. P. McCLYMER and M. M. LABES

Department of Chemistry, Temple University, Philadelphia, PA 10122

Magnetic field induced reorientation of a nematic liquid crystal can be accompanied by a transient periodic deformation pattern. The dynamics of the formation and decay of this deformation are studied in the lyotropic nematic phase of disodium cromoglycate (DSCG) in water utilizing computer-assisted imaging techniques. The early time behavior is well-described by linearized nemato-hydrodynamic equations, while the long time behavior shows a rich variety of structures.

INTRODUCTION

Realignment of liquid crystals by viscous flow, or electric or magnetic torques, is accompanied by spatial non-equilibrium transient order that is an example of the general phenomenon of spontaneous dynamic periodic structures.[1-3] Such magnetically induced periodic responses have been found for all classes of nematics.[4-9] The lifetime of the structure in thermotropics is very short, while lyotropic and polymeric nematics exhibit a long-lived, fully developed pattern that can be examined in detail.[10]

The periodic response is brought about by the degeneracy of the director, the free energy of the nematic being the same for n as for $-n$. This degeneracy allows the formation of counter rotating regions which reduce the effective rotational viscosity, which in turn allows the periodic response to develop faster than the uniform response.[8] The nonlinearity of the system causes the fastest response to quickly dominate and manifest itself macroscopically. A quantitative treatment has been developed by using linearized versions of the nemato-hydrodynamic equations and applying suitable boundary conditions.[4,8,10,11] The periodic response is caused by a competition between the elastic energy of the deformation and the spatial dependence of the reduced viscosity, and is predicted in terms of material parameters, external field, and cell thickness. Studies to date have concentrated on measuring the statics of the periodic pattern and the results have been in good agreement with theory.[4,8,10–13] However, the theory also predicts that the pattern should grow exponentially in time for small deformations. We report here the results of studying the time dependence of the growth of the deformation.

EXPERIMENTAL

A lyotropic nematic formed from 13.5% DSCG and water is a particularly convenient system to study.[7,10,12,13] DSCG is provided by Fisons Pharmaceuticals Inc. and is used without further purification. Samples are placed into thin capillary cells, 0.2 × 4 × 20 mm which are sealed with a microtorch. The sample cell is placed into a temperature controlled housing attached to a rotation stage in between the pole faces of an electromagnet. Figure 1 shows the sample fixed coordinate system used in this experiment. The long axis of the cell, the x axis, is initially parallel to the vertical direction and perpen-

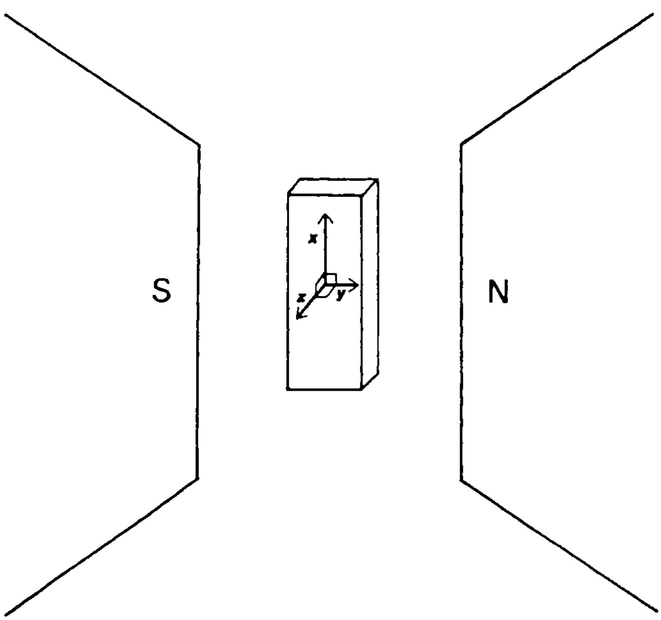

FIGURE 1 Coordinate system used in the experiment.

dicular to the applied magnetic field. The DSCG lyophase has a negative diamagnetic anisotropy and thus the director aligns perpendicularly to the magnetic field. The director prefers to lie in the xz plane because of the shape anisotropy of the capillary. The alignment is induced by a 20 KG field applied overnight and is checked visually through crossed polarizers.

Reorientation of the nematic director is induced by rotating the x axis so that it is now parallel to the magnetic field. This procedure is performed manually and takes about half a second. The free energy is reduced by director motion that places the director perpendicular to the field, along y or $-y$. Deformation along the z axis has also been reported and is manifested by the formation of nodes along the stripes.[7,10] Except for this node region, the distortion is uniform along z.

The distortion is viewed with a high resolution black and white RCA camera attached to a Kataptaron (H and R Optical) long working distance microscope which is about 1 meter from the sample. Total magnification of both the microscope and the camera is 58. The output of the camera is digitized (512×512 pixels, 256 gray levels) and stored in a computer.

Some difficulties arise with the use of a standard vidicon which can easily be remedied. These types of cameras are meant to be used with video monitors and thus have a nonlinear light response to match the monitors. Additionally, the camera has a large dynamic range that is brought about by varying the voltage across the vidicon tube as a function of light intensity. For use in this experiment, "autotargeting" is defeated and the tube output linearized over the observable range. Vidicons also show nonuniform response which can be seen by viewing the width of the histogram of the camera output when the camera is illuminated with (nearly) uniform light. The width of the histogram is also a function of vidicon voltage. With the settings used for this experiment, the full width at half maximum is 8 pixels. As with other detectors, the vidicon dark count is both voltage and temperature dependent. Temperature effects are reduced by allowing the camera to warm up for a number of hours and keeping the room temperature fairly constant.

The light source is a 150 watt halogen bulb attached to a fiber optical cable. A lens mount is attached to the fiber cable to reduce spreading of the beam. The output passes through a ground glass diffusion plate and then a polarizer with optic axis parallel to the vertical, along the initial director. The beam is further focussed and passes through the sample and a crossed analyzer and is then viewed with the microscope. Birefringence of the sample is very low, so that at the thickness employed the optical path difference for all visible wavelengths is less than λ/4. This can be verified by rotating an aligned sample from 0° to 45° while observing with 400 nm light. The intensity of the transmitted light was found to monotonically increase with angle.

The intensity of the transmitted light is given by

$$I = I_0 \sin^2(\theta) \cos^2(\theta) + I_{\text{dark}} \tag{1}$$

where θ is the distortion angle given by

$$\theta = \theta_0 \, e^{st} \cos(q\, x) \tag{2}$$

and s and q are the growth rate and wave vector respectively. I_0 is determined by observing I when a uniformly aligned sample is rotated 45°. I_0 is then $4 \times I_{45}$. In this way, intensity information is utilized as a measure of the absolute deviation angle.

Owing to limitations in storage capacity and speed of a hard disk, only ⅛ of the picture (128 × 256 pixels) is stored. At the conclusion of data acquisition, the computer converts intensity information into deviation angle, and Fourier transforms this information to determine

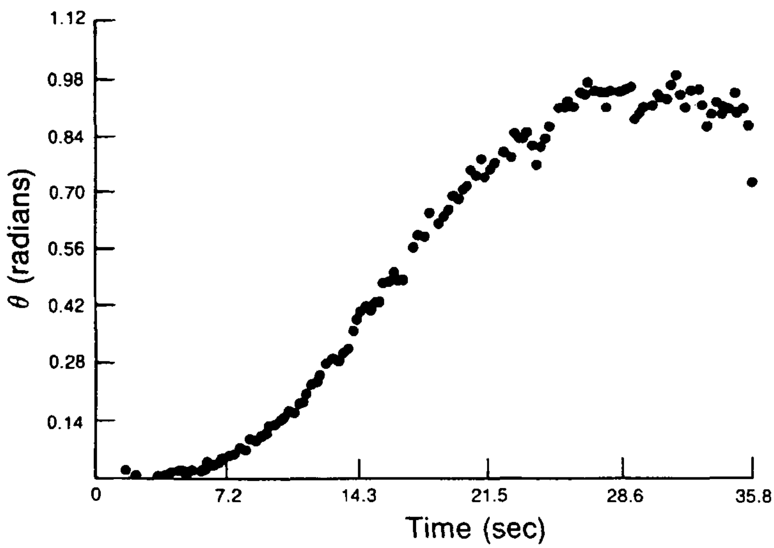

FIGURE 2 Temporal behavior of the dominant Fourier mode, converted to distortion angle.

the growth rate of the varius growth modes. The process is repeated for 100 scan lines to improve statistics. For technical reasons, the use of a window function can improve the resolution and sensitivity of the transform, and for this work we use a Hamming window.[14]

RESULTS

Surprisingly, the growth rate is found to be position dependent. We do not believe this to be an effect of the reorientation phenomena but an experimentally induced effect. Over the small viewing range (8 mm), the growth rate is faster further from the nematic/air inter-

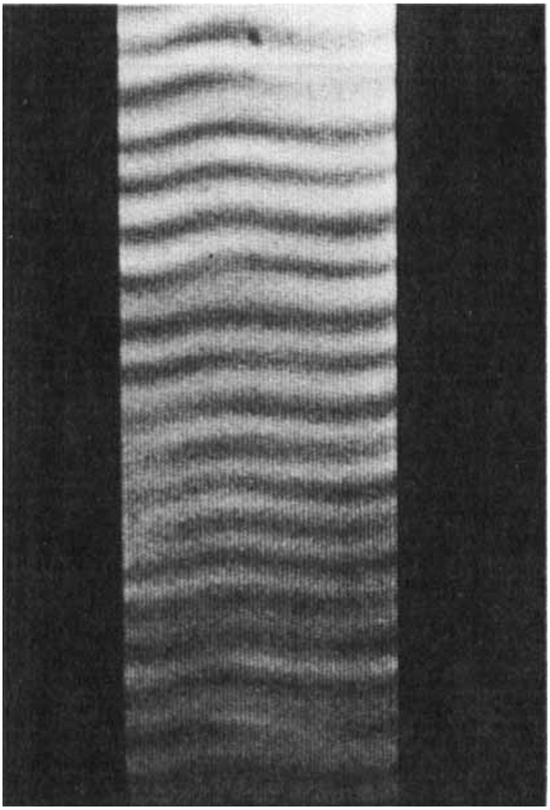

FIGURE 3 Time evolution of the periodic response at 6.05 KG. (a) 75 seconds; (b) 135 seconds—the blurring together of the stripes can be seen; (c) 160 seconds—alternating bright and dark stripes can be seen at the top of the photograph while the pairing of lines is seen on the bottom.

face, which is about 1 cm away. The large distance from the meniscus would seem to rule out static boundary effects. Rotation of the cell from a vertical to a horizontal configuration should cause flow near the meniscus that could disturb the reorientation process. Fortunately, the stored region shows mostly uniform growth. Deviations at the edge are reduced by the window function that reduces edge contributions to zero. The net result is to reduce the effect of the anisotropic growth rate allowing meaningful measurements, which we report below.

Figure 2 shows the temporal behavior of the dominant growth mode at 6.05 KG. The wavelength of the distortion, 100 μm, is in good agreement with published results. The deviation angle is calculated from the magnitude of the Fourier component using the Hamming

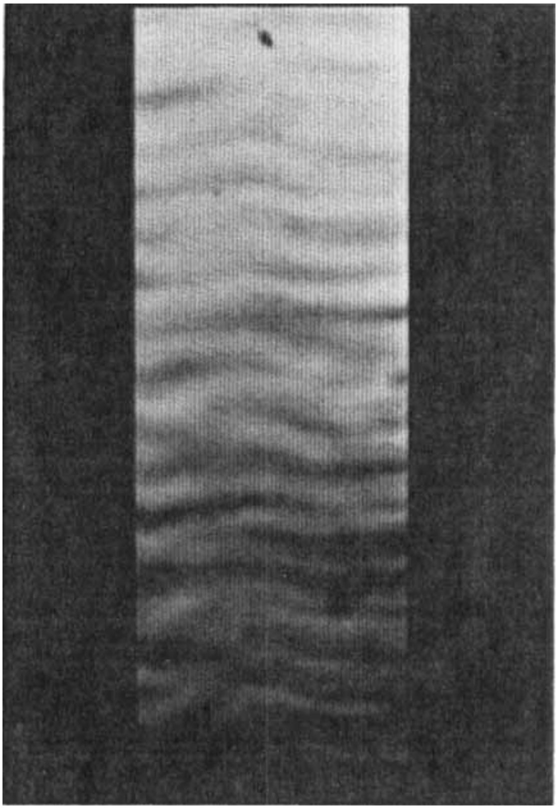

FIGURE 3b

window function. Maximum transmitted light is expected when the reorientation angle is 45°. This angle can be identified with the plateau in the Figure and allows a comparison of the measured values with the true distortion angle. Agreement is about 15%, near the expected accuracy.

The early time behavior is nearly exponential. The sum of residuals of computer fits to subsets of the data start to increase quickly at about 14 seconds. This value sets an upper limit of about 12° on the distortion angle that is still well described by the linearized equations. At the other extreme, a good exponential can be drawn up to about 9 seconds at which time the distortion angle is 6°. Extreme deviations are seen for the earliest times, up to 4 seconds as a result of the very small signal to noise ratio. We know, however, that the y intercept

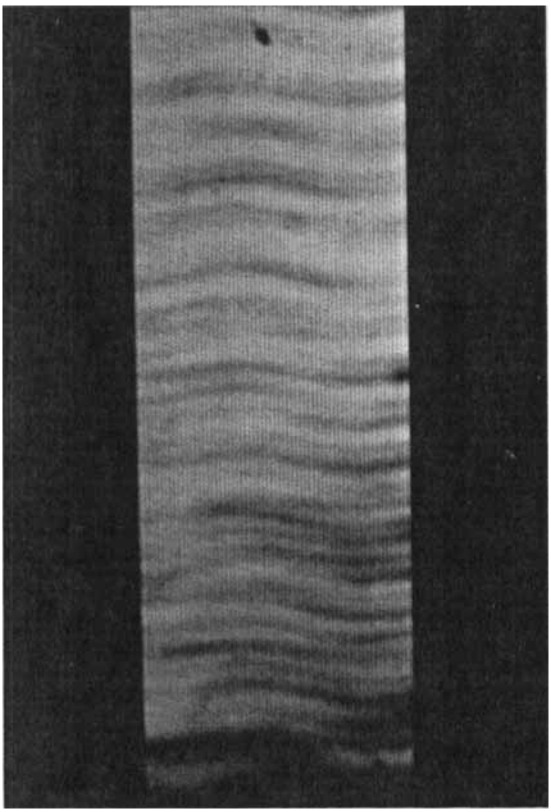

FIGURE 3c

must occur near time = 0, since this is the value of thermally induced director fluctuation.

The long time behavior of the system turns out to be surprisingly complicated, as is shown in the photographs in Figure 3. For the 6.05 KG field, the pattern goes through three stages during the observation period, about 170 seconds. The initial pattern is the growth of evenly spaced bright lines. These lines brighten and meld together to form a nearly homogeneous bright region. This process is noticeable at 50 seconds and continues until about 120 seconds. At this point, the distinct lines start to become visible to reveal a doubling up of bright lines separated by a thin dark line. The pairs themselves are separated by a thicker dark line. At 150 seconds, the pattern then changes to a series of bright lines and less bright lines. Another sample at 4 KG showed similar behavior with the darker lines brightening as the bright lines darkened until the relative brightnesses were switched. This behavior is not universal. The same sample at 5 KG showed a blurring together of the lines and then a separation into broad bright lines separated by darker narrow lines. This complicated behavior is not predicted by the linearized analysis. The complicated temporal behavior must be due to either the nonlinear interactions predicted by the hydrodynamic equations, or be a result of the anisotropic growth rate. The latter explanation is being investigated by keeping the sample in the horizontal plane to eliminate rotationally induced flow which might be the cause of the anisotropic growth rates.

CONCLUSION

The dynamics of the growth process are well described by linearized nematohydrodynamics for even fairly large distortion angles (up to 12°). The initial periodicity of the distortion is time independent and is in good agreement with other published results. Long time behavior exhibits an unexpectedly rich variety of patterns. The source of these time varying patterns is not clear, and further work is underway to clarify the problem.

Acknowledgment

This work was supported by the National Science Foundation—Solid State Chemistry under Grant No. DMR84-04009.

References

1. G. Nicolis and I. Prigogine, "*Self Organization in Nonequilibrium Systems*," John Wiley & Sons, New York, 1977.
2. J. Ross, *Ber Bunsenges.*, *Phys. Chem.*, **80**, 1112 (1976).
3. D. A. Huberman, *J. Chem. Phys.*, **65**, 2013 (1976).
4. F. Lonberg, S. Fraden, A. J. Hurd and R. B. Meyer, *Phys. Rev. Lett.*, **52**, 1903 (1984).
5. J. Charvolin and Y. Hendrikx, *J. Phys. Lett.*, **41**, 597 (1980).
6. L. J. Yu and A. Saupe, *J. Am. Chem. Soc.*, **102**, 4879 (1980).
7. H. Lee and M. M. Labes, *Mol. Cryst. Liq. Cryst.*, **84**, 137 (1982).
8. E. Guyon, R. Meyer and J. Salan, *Mol. Cryst. Liq. Cryst.*, **54**, 261 (1979).
9. E. F. Carr, *Mol. Cryst. Liq. Cryst. Lett.*, **34**, 159 (1977).
10. Y. W. Hui, M. R. Kuzma, M. San Miguel and M. M. Labes, *J. Chem. Phys.*, **83**, 288 (1980).
11. A. J. Hurd, S. Fraden, F. Lonberg and R. B. Meyer, *J. Phys.*, (Paris) **46**, 905 (1985).
12. D. V. Rose and M. R. Kuzma, *Mol. Cryst. Liq. Cryst. Lett.*, in press (1986).
13. M. R. Kuzma, *Phys. Rev. Lett.*, **57**, 349 (1986).
14. Robert W. Ramirez, "*The FFT, Fundamentals and Concepts*," Prentice Hall, Englewood Cliffs, New Jersey (1985).